Veterinary Microbiology 239 (2019) 108485

Contents lists available at ScienceDirect

Veterinary Microbiology

journal homepage: www.elsevier.com/locate/vetmic

Induction of the unfolded protein response (UPR) during pseudorabies virus infection

Songbai Yang[1], Jingjing Zhu[1], Xiaolong Zhou, Han Wang, Xiangchen Li, Ayong Zhao*

Key Laboratory of Applied Technology on Green-Eco-Healthy Animal Husbandry of Zhejiang Province, College of Animal Science and Technology, Zhejiang A&F University, Hangzhou, China

ARTICLE INFO

Keywords:
PRV
ER stress
UPR
GRP78
IRE1
XBP1

ABSTRACT

Pseudorabies virus (PRV) infection causes great economic losses in the pig industry. By disrupting the homeostasis of the endoplasmic reticulum (ER), many viral infections induce ER stress and trigger the unfolded protein response (UPR). However, the roles of ER stress and UPR in PRV infection remain unclear. In the present study, we demonstrate that the expression of the ER stress marker glucose-regulated protein 78 (GRP78) increased during the early stages of PRV infection, indicating that ER stress was induced. Examination of the three branches of the UPR revealed that the IRE1-XBP1 and eIF2α-ATF4 pathways were activated during PRV infection. In addition, PRV induced apoptosis in later stages of infection through the CHOP-Bcl2 axis. Overexpression of GRP78 or ER stress inducer treatment with thapsigargin could enhance PRV production. Conversely, ER stress inhibitor treatment with tauroursodeoxycholic acid reduced PRV replication. Taken together, our results reveal that PRV infection induces ER stress and activates the IRE1-XBP1 and eIF2α-ATF4 pathways.

1. Introduction

Pseudorabies virus (PRV), also called Suid herpesvirus 1 (SuHV-1), belongs to family *Herpesviridae*. The genome of PRV is linear double-stranded DNA, approximately 143 kb in size, contains more than 70 genes (Klupp et al., 2004). PRV can infect a variety of livestock and wild animals and causes acute infectious diseases with encephalomyelitis as the main symptom. The pig is the only natural host of PRV, and PRV can cause porcine Aujeszky's disease (AD), an important swine disease (Pomeranz et al., 2005). PRV can also cause nervous and respiratory system disorders in newborn piglets and reproductive failure in sows, resulting in great economic losses in the pig industry (Klupp et al., 2004). Because of improved protective measures and the widespread use of vaccines in some European countries, including Norway, Finland, and Belgium, pseudorabies has been largely eliminated in some farms; however, PRV still exists in wild boars, so the possibility of recurrence of this disease persists in these areas (Muller et al., 2011; Verpoest et al., 2014). Additionally, in 2012–2013, a sudden outbreak of pseudorabies caused by a highly virulent mutant PRV strain in China caused substantial economic losses to the pig industry (Gu et al., 2015; Yu et al., 2014). Therefore, to identify the host factors that aid in PRV resistance, the mechanisms of the regulation of host factors involved in PRV replication need to be further studied.

The endoplasmic reticulum (ER) is a multifunctional cellular organelle that is involved in the synthesis, folding and trafficking of proteins. An overabundance of proteins or accumulation of misfolded proteins in the ER will cause ER stress; in response, cells activate the unfolded protein response (UPR) to restore ER homeostasis (Schroder and Kaufman, 2005; Walter and Ron, 2011). To date, three main branches of the UPR have been identified. These three branches are mediated by three ER-resident transmembrane signaling sensors: IRE1 (inositol requiring enzyme 1), PERK (PKR-like ER protein kinase), and ATF6 (activating transcription factor 6) (Ron and Walter, 2007; Walter and Ron, 2011). Under normal conditions, these three signaling proteins are bound by glucose-regulated protein 78 (GRP78), a molecular chaperone, maintaining the UPR in an inactive state. When unfolded or misfolded proteins accumulate in the ER, the UPR is activated. Initially, GRP78 is released from the three sensors; while GRP78 then binds the unfolded or misfolded proteins to regulate their folding and decreases protein translation (Ibrahim et al., 2019; Zhang et al., 2017), the three activated sensors trigger a complex signal transduction cascade.

When IRE1 is activated, it dimerizes and autophosphorylates, resulting in activation of its endoribonuclease activity. Activated IRE1 cleaves a 26-base intron segment of the X-box binding protein 1 (XBP1)

* Corresponding author.
E-mail address: zay503@zafu.edu.cn (A. Zhao).
[1] These authors contributed equally to this work.

https://doi.org/10.1016/j.vetmic.2019.108485
Received 19 July 2019; Received in revised form 25 October 2019; Accepted 25 October 2019

Table 1
Primers used in this study.

Genes	Sequence (5'-3')	TM (°C)	Size (bp)	Application
ATF4	F: TGGAGCAGAACAAGACAGC R: CTTTACATTCGCCAGTGAG	60	81	qPCR
CHOP	F: ACCTTCACCACTCTTGACCCTG R: TGCTTGAGCCGTTCGTTC	60	275	qPCR
Bcl-2	F: ACACTGCCATTCCGTTTC R: TCACTTTGTCCACCTCCA	60	81	qPCR
GRP78	F: TCTACTCGCATCCCAAAG R: CTCCCACGGTTTCAATAC	60	199	qPCR
IRE1	F: GGACTGGCGGGAGAACAT R: CGTGGTAGTAGGGCTGGAA	60	272	qPCR
XBP1	F: GGATTCTGACGGTGTTGA R: GGAGGCTGGTAAGGAACT	60	161	qPCR
(u/s)XBP1	TGCCTTAGTTACTGAAGAGGA CAGAATGCCCAAGAGGATA	60	178/204	RT-PCR
GAPDH	F: GGACTCATGACCACGGTCCAT R: TCAGATCCACAACCGACACGT	60	220	qPCR/ RT-PCR
PRV-gE	F: CCGAGGACGAGTTCAGCA R: GGCCCATTCGTCACTTCCG Probe: FAM-ACCAGACGTCGAAGCCGGA-BHQ1	60	121	qPCR
GRP78	F: CGGGATCCCGATGAAGCTGTCCCTGGTGG R: CCGCTCGAGCGGCTACAACTCATCTTTGTCTG	60	1987	Cloning

F: forward primer, R: reverse primer, the enzyme cleavage site and protective base were underlined.

mRNA, resulting in spliced XBP1. Spliced XBP1 is transported to the nucleus as a transcription factor and upregulates genes that are responsible for protein folding and the ER-associated protein degradation (ERAD), thereby restoring ER homeostasis (Lee et al., 2003; Zhang and Kaufman, 2004). When ER stress is severe and cannot be restored, the UPR can induce apoptosis (Tabas and Ron, 2011). When the PERK pathway is activated, PERK oligomerizes and autophosphorylates, which results in the phosphorylation of the eukaryotic translation initiation factor 2 subunit (eIF2α), leading to mRNA translation inhibition. In addition, the translation of the activating transcription factor ATF4 can be enhanced, which then upregulates CHOP to induce apoptosis (Walter and Ron, 2011). In response to ER stress, activated ATF6 is transported into the Golgi apparatus where it is cleaved by site 1 proteases (S1P) and site 2 proteases (S2P) to release ATF6 with an active N-terminal DNA-binding domain [ATF6(N)]. ATF6(N) enters the nucleus and upregulates the expression of molecular chaperone-related proteins, such as GRP78 and GRP94, to help the ER restore homeostasis (Ron and Walter, 2007; Walter and Ron, 2011).

Viral infection can also activate autophagy through the UPR pathways (Cai et al., 2016; Sharma et al., 2017). Previous studies have found that PRV induces and inhibits autophagy during the early and late periods of infection in different cell lines (Sun et al., 2017), and PRV-induced autophagy enhances viral replication in mouse neuro-2a cells (Xu et al., 2018). Using proteomic analysis, our previous research showed that a group of genes involved in ER stress is upregulated in PRV-infected PK15 cells (Yang et al., 2017). We speculated that PRV infection induced ER stress to activate UPR. However, it remains unclear which of the UPR sensors is involved and what roles the three UPR pathways play in PRV infection. In this study, we showed that ER stress was induced in PRV-infected PK15 cells, and our examination of the expression of the three UPR sensor genes revealed that the IRE1-XBP1 and eIF2α-ATF4 pathways were activated during PRV infection. Additionally, overexpression of GRP78 increased viral yield. Finally, using chemicals to modulate ER stress, we also found that the ER stress induced by PRV infection could promote PRV replication. These results promote our understanding of PRV-UPR interactions.

2. Materials and methods

2.1. Cells, viruses, and infection

Porcine kidney epithelial PK15 cells were grown in Modified Eagle Medium (MEM) (HyClone, South Logan, UT, USA), supplemented with 10 % fetal bovine serum (FBS) (HyClone) and 1 % nonessential amino acids (Gibco, Grand Island, NY, USA), and maintained in a humidified incubator at 37 °C and 5 % CO_2. The virulent wild-type PRV strain ZJ (Zhejiang) was utilized in this study (Yang et al., 2017). Virus titers were measured using 50 % tissue culture infectious dose (TCID50) in PK15 cells and analyzed using the Reed-Muench method.

Monolayers of confluent PK15 cells were seeded in the wells of a 12-well cell culture plate. When the cells reached 90 % confluence, they were washed twice with phosphate buffer saline (PBS). Then, the cells were infected with PRV (5 μL of $10^{-6.625}$ TCID50/0.1 mL per well) diluted in MEM. After 1 h of adsorption, the infected cells were washed three times with PBS and then maintained in MEM supplemented with 2 % FBS and 1 % nonessential amino acids. The infected cells and supernatant were collected for the determination of viral replication and titer, respectively, at the indicated time points post-infection.

2.2. Antibodies and reagents

The following primary antibodies were used in our study: GRP78 (Proteintech, 11587-1-AP; 1:1000), IRE1 (Bioss, bs-8680R; 1:500), p-IRE1 (Abcam, ab48187; 1:1000), ATF6 (Abclonal, A0202; 1:1000), p-eIF2α (phospho-S51) (Abcam, ab32157; 1:500), eIF2α (Bioworld, BS3651; 1:500), pseudorabies virus (Thermo Fisher, PA1-081; 1:1000), and β-Actin (Proteintech, 60008-1-Ig; 1:5000). The secondary antibodies used were goat anti-rabbit IgG-HRP (Abbkine, A21020; 1:5000) and goat anti-mouse IgG-HRP (Abbkine, A21010; 1:5000) purchased from Abbkine Company. The ER stress inhibitor tauroursodeoxycholic acid (TUDCA) (Merck-Millipore, 580549-1GM) and inducer dithiothreitol (Cell Signaling Technology, 7016 L) were dissolved in sterile water. The ER stress inducer thapsigargin (MedChem Express, HY-13433) was dissolved in dimethyl sulfoxide (DMSO).

2.3. Quantitative-PCR (qPCR) analysis of UPR gene expression and PRV replication

To examine the expression of UPR genes, total RNA was isolated using TRIzol reagent (Thermo Fisher, Waltham, MA, USA) according to the manufacturer's instructions. cDNA was synthesized from 1 μg of total RNA using the RT-PCR reagent kit (Cwbiotech, Beijing, China). Real-time quantitative PCR was performed on a CFX96 Touch instrument (Bio-Rad) using SYBR Green PCR master mix (Takara, Dalian,

China). The qPCR primer sequences are listed in Table 1. The PCR program was as follows: 95 °C for 2 min, followed by 40 cycles of 95 °C for 5 s, 60 °C for 30 s, and 72 °C for 15 s, followed by melting curve analysis. Relative expression levels were calculated by using the $2^{-\Delta\Delta Ct}$ method using GAPDH as the reference gene (Livak and Schmittgen, 2001). To quantify viral replication, the copy number of PRV gE gene was analyzed using absolute quantification real-time PCR. Briefly, after infection with PRV for indicated periods of time, the total DNA of the infected cells was isolated by the phenol-chloroform extraction method. The primers and the probe used to detect PRV replication are listed in Table 1. For the standard sample, the gE gene was amplified and cloned into the pMD-19 T vector (Takara, Dalian, China). A standard curve of CT values versus gE copy number was constructed from qPCR data using 10-fold serial dilutions of the pMD-gE vector. The gE copy numbers in samples from the experiments were determined using the CT value and the linear equation from the standard curve.

2.4. RT-PCR analysis of XBP1

Total RNA was extracted from PRV-infected or uninfected PK15 cells using TRIzol reagent. Reverse transcription was carried out and then PCR was performed with Taq MasterMix (Cwbiotech, Beijing, China) using the primers listed in Table 1. Electrophoresis on a 2 % agarose gel was used to resolve the resulting PCR products, with fragments of 204 bp and 178 bp representing unspliced XBP1 (uXBP1) and spliced XBP1 (sXBP1), respectively.

2.5. Western blotting

Cells were lysed using RIPA lysis buffer supplemented with phosphatase and protease inhibitor cocktails (Cwbiotech, Beijing, China). Equal amounts of total cell lysates were separated by SDS-PAGE and transferred to polyvinylidene difluoride (PVDF) membranes (Millipore, Billerica, MA, USA). The membranes were blocked with 5 % nonfat milk in Tris-buffered saline containing 0.1 % Tween-20 (TBST) and were then incubated with primary antibodies overnight at 4 °C. Membranes were then washed three times and incubated with a horseradish peroxidase-conjugated secondary antibody for 1 h at ambient temperature. Finally, the membranes were treated with Immobilon Western Chemiluminescent HRP Substrat (Merck Millipore, Darmstadt, Germany), using β-actin as an internal control, and imaged under a Tanon 5200 system (Biotanon, Shanghai, China). The mean densities of the protein bands were measured using ImageJ software.

2.6. Plasmid construction, siRNA knockdown and transfection

The coding sequence (CDS) of porcine GRP78 was amplified using primers flanked by BamHI/XhoI sites (Table 1) and cloned into the pcDNA3.1 vector to generate the pcDNA3.1-GRP78 plasmid. siRNAs against GRP78, IRE1, and XBP1, along with control scrambled siRNA, were synthesized by Genepharma (Shanghai, China). The siRNA sequences are listed in Table 2. PK15 cells were cultured in a 12-well plate. PcDNA3.1-GRP78, targeted siRNA, and control scrambled siRNA were transfected into the cells using Lipofectamine 3000 transfection reagent (Invitrogen, Carlsbad, CA). At 48 h post-transfection, cells were either harvested for RNA and protein extraction or were infected with PRV for an additional period of time and then harvested at indicated time points for the detection of viral replication and virus titration.

Table 2
Sequences of sense strands of siRNA used in this study.

Genes	Sequence (5'-3')
GRP78(pool)	CCUUCUCACCAUUGAUAAUTT
	GCUGGAAGAUUCUGAUUUATT
	GCCUCUGAUAAUCAGCCAATT
IRE1	CCAUCAUCCUGAGCACCUUTT
XBP1	CCAGUCAUGUUCUUCAGAUTT
scrambled	UUCUCCGAACGUGUCACGUTT

2.7. Assay for cell viability

Cell viability was assessed by the CCK-8 assay kit (Beyotime, Shanghai, China). Cells were cultured in 96-well plates for 24 h. The medium was then replaced with MEM medium containing the indicated concentrations of thapsigargin (Tg) or tauroursodeoxycholic acid (TUDCA). The cells were cultured for additional periods of time, as indicated. Next, the medium was removed, and the cells were washed twice with PBS. The cells were then incubated with 100 μL of fresh medium containing 10 μL of the CCK-8 reagent for 4 h at 37 °C, after which the optical density was measured at 450 nm using an iMARK microplate reader (Bio-Rad).

2.8. Statistical analysis

All data are presented as the mean ± standard error (SE) of 3 (qPCR) or 2 (TCID50 assays) independent experiments. Statistical significance was assessed by Student's t-test, and statistical significance was ascribed at $p < 0.05$ (*) and $p < 0.01$ (**).

3. Results

3.1. Growth kinetics of PRV in PK15 cells

The PK15 cell line is a suitable model for PRV infection in many studies. To determine the growth kinetics of PRV in PK15 cells and the optimal infection time point for viral propagation analysis, PK15 cells were infected with PRV and then examined for cytopathogenic effect (CPE), viral genome replication and viral titers at indicated post-infection time points. From 2–24 h post-infection (hpi), progressively more dead cells floated in the medium compared to uninfected cells; additionally, the CPE became readily apparent as the infection progressed (Fig. 1A). Obvious visible CPEs were observed at 24 hpi, including cell rounding, swelling, cell detachment, and severely diseased cell morphology (Fig. 1A). Viral genome replication was monitored using absolute qPCR, and the results showed that the viral genome replication in PK15 cells peaked at 24 hpi (Fig. 1C). The viral yield also peaked at 24 hpi (Fig. 1D). In contrast, no obvious CPE was observed in the PK15 cells at 12 hpi despite the viral replication remaining high. Therefore, the time point of 12 hpi was chosen for viral propagation analysis.

3.2. PRV increased GRP78 expression during early infection

In response to ER stress, GRP78 is released from the UPR sensors and then binds and corrects unfolded or misfolded proteins, resulting in UPR activation. Therefore, induction of GRP78 expression has been used as an ER stress marker (Lee, 2005). To determine whether PRV infection induces ER stress, PK15 cells were infected with PRV, then the cells were harvested at indicated time points post-infection. The expression of GRP78 was examined by qRT-PCR and western blotting. The results showed that GRP78 mRNA and protein levels were persistently upregulated from 2 to 8 hpi compared to mock-infected cells (Fig. 2). However, the expression of GRP78 decreased from 12–24 hpi (Fig. 2). Thus, these results demonstrated that PRV potentially induced ER stress at early infection stages.

3.3. PRV infection activated the UPR via the IRE1-XBP1 and eIF2α-ATF4 pathways

To determine whether PRV infection activated the UPR pathways, PK15 cells were infected with PRV. After infection, at the indicated time

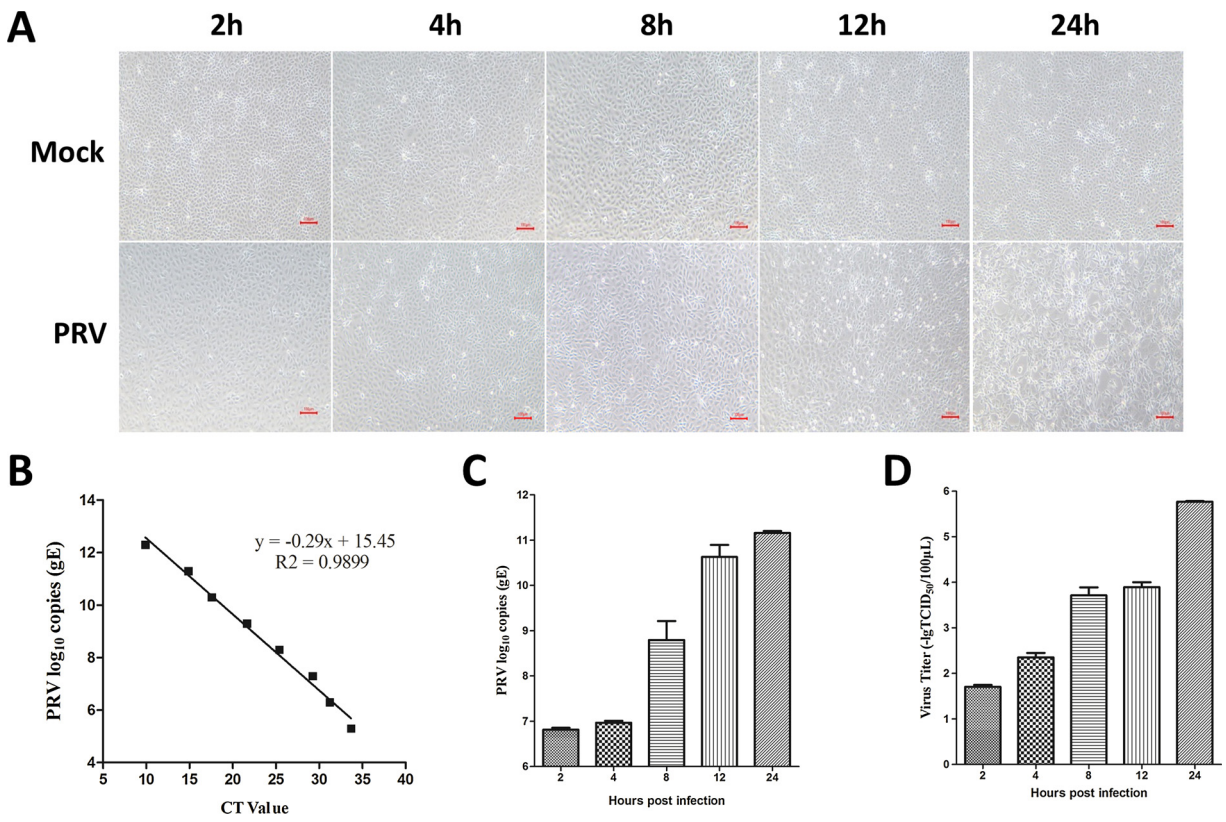

Fig. 1. Kinetics of PRV propagation in PK15 cells. (**A**) Morphological changes in PK15 cells at 2, 4, 8, 12, and 24 h after PRV infection, with mock-infected cells as a control. (B) Standard curve for absolute qPCR. Confirmation of the viral replication (C), measured by absolute qPCR, and virion production (D), assessed by titer determination methods, in PRV-infected PK15 cells at 2, 4, 8, 12, and 24 h.

points, the cells were harvested, total RNA and proteins were extracted. The expression of UPR-related genes was examined using qRT-PCR and western blotting. The results showed that the protein levels of phosphorylated IRE1 were slightly and transiently decreased at 2 hpi and then were persistently increased from 4 to 24 hpi compared to the levels in mock-infected cells (Fig. 3A). Activated IRE1 uses its endoribonuclease activity to cleave a 26-base intron segment of the XBP1 mRNA to form sXBP1, and sXBP1 activates the transcription of genes to enhance cellular protein-folding capacity (Calfon et al., 2002). Therefore, the levels of uXBP1 and sXBP were analyzed during PRV infection. The XBP1 cDNA was amplified using RT-PCR and resolved by electrophoresis on a 2 % agarose gel. The results showed that sXBP1 levels were upregulated immediately after PRV infection, and this upregulation lasted until 24 hpi. Meanwhile, the levels of uXBP1 were decreased (Fig. 3C). These results indicated that the IRE1-XBP1 pathway was activated during PRV infection. In addition, to determine the roles of the IRE1-XBP1 pathway in PRV infection, siRNAs were used to knockdown the expression of IRE1 and XBP1 (Supplemental Fig. 1A, C). Knockdown of IRE1 or XBP1 expression did not significantly affect PRV infection (Supplemental Fig. 1B, D).

Dissociation of GRP78 from PERK initiates PERK dimerization and autophosphorylation. Activated PERK phosphorylates eIF2α to attenuate mRNA translation (Walter and Ron, 2011). To determine whether the PERK pathway was activated by PRV infection, cells were harvested at indicated time points following PRV infection and total RNA and proteins were isolated. Western blotting showed that the levels of phosphorylated eIF2α were up-regulated at 2 hpi and 24hpi and were slightly decreased from 4 to 12 hpi compared to the levels in mock-infected cells (Fig. 3A). We could not find suitable antibodies for porcine PERK. However, p-eIF2α can increase translation of ATF4 mRNA and subsequently activate CHOP transcription by binding its promoter to induce cell apoptosis (Oyadomari and Mori, 2004); therefore, we analyzed the expression of ATF4 and CHOP during PRV infection by qRT-PCR. The results showed that PRV infection significantly upregulated the expression of ATF4 and CHOP (Fig. 3D). The expression of Bcl-2, a gene regulated downstream of CHOP, was downregulated at 24 hpi (Fig. 3D). These results demonstrated that PRV infection might activate the PERK-eIF2α-ATF4-CHOP-Bcl-2 pathway. Alternatively, the activation of IRE1 can also lead to transcriptional activation of CHOP (Fribley et al., 2009). Therefore, siRNAs were used to knockdown the expression of IRE1 and XBP1, respectively, and then infected with PRV. At 12 hpi, the CHOP expression was examined by qPCR. The results showed that the CHOP expression did not significantly changed after IRE1 or XBP1 knockdown during PRV infection, which implied that IRE1-XBP1 activation was not reponsible for increased CHOP expression (Supplemental Fig. 2). In addition, another UPR sensor, ATF6, was not activated after PRV infection, as cleaved ATF6 could not be detected (Fig. 3A).

3.4. Overexpression of GRP78 facilitated PRV replication

GRP78 is an important regulator of the UPR, and virus-induced GRP78 expression modulates viral replication (Zhou et al., 2016). To identify the role of GRP78 in PRV infection, GRP78 was overexpressed in PK15 cells via transfection with the recombinant eukaryotic vector pcDNA3.1-GRP78. At 48 h post-transfection, total RNA and protein were extracted. The expression of GRP78 was examined by qRT-PCR and western blotting (Fig. 4A, B). The results showed that GRP78 was significantly overexpressed in pcDNA3-GRP78-transfected cells compared to cells transfected with the pcDNA3.1 empty vector. Next, PK15 cells were transfected with the pcDNA3.1-GRP78 vector and then infected with PRV for 12 h. The DNA of the cells was extracted for absolute qPCR, and the supernatant was harvested for TCID50 assays (Fig. 4C, D). The results showed that overexpression of GRP78

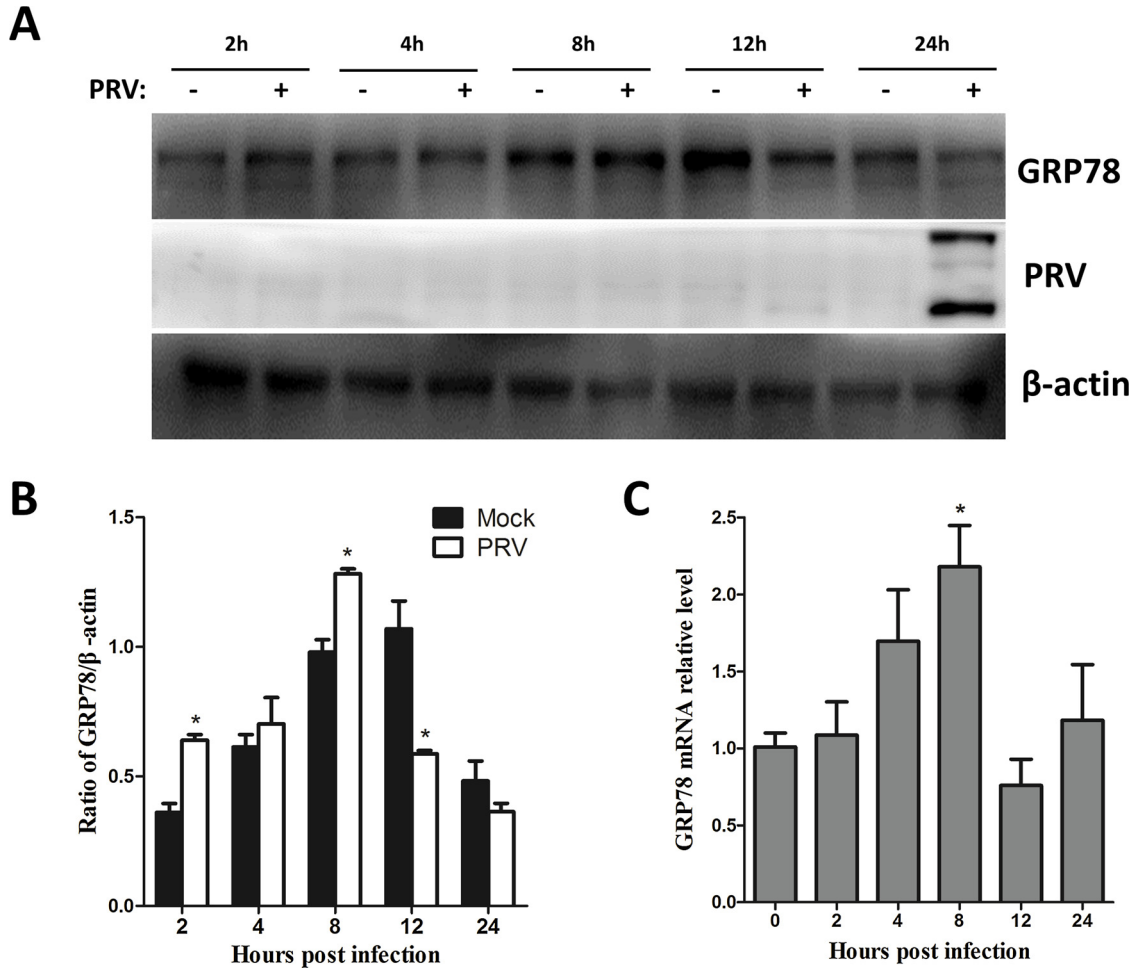

Fig. 2. The expression of GRP78 is upregulated during early PRV infection. (A) PK15 cells were infected with PRV for 2, 4, 8, 12 h, and 24 h. The expression of GRP78, assessed by western blotting. Mock-infected cells were used as controls. (B) The expression levels of GRP78 relative to β-actin levels, analyzed through densitometric scanning. (C) PK15 cells were infected with PRV for indicated periods of time and the mRNA level of GRP78 was examined by qRT-PCR analysis.

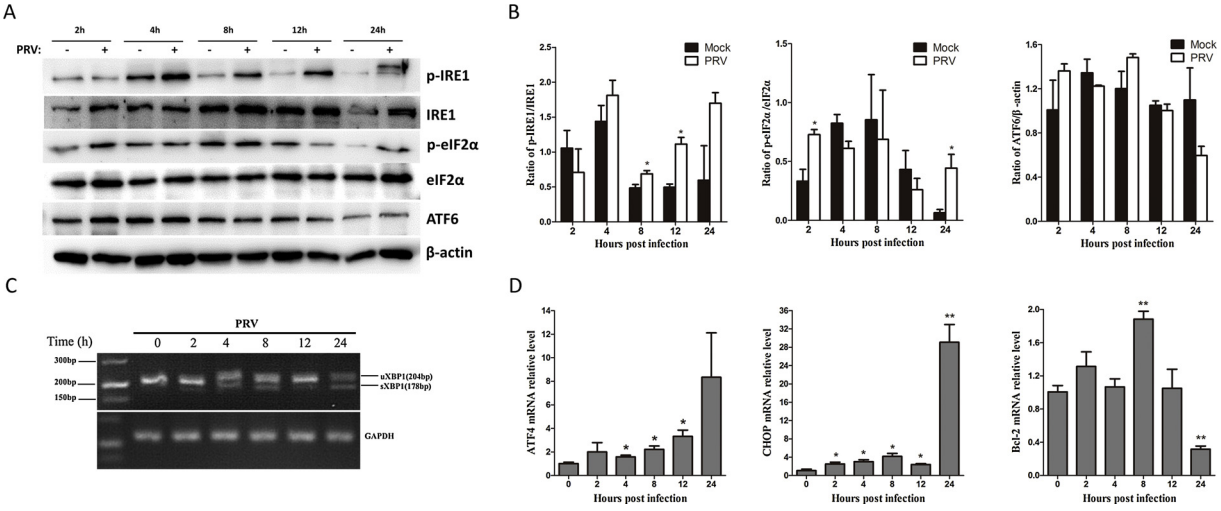

Fig. 3. PRV infection induces the activation of UPR and expression of the proapoptotic protein CHOP. PK15 cells were infected with PRV or were mock-infected for indicated periods of time. (A) Western blot analysis of the indicated target proteins of UPR signaling pathways during PRV infection, with mock-infected cells as controls. (B) The quantitation of protein levels from (A). β-Actin was used as a loading control. (C) Splicing levels of XBP1 mRNA, analyzed by RT-PCR as described in Materials and methods using total RNA extracted from PRV-infected PK15 cells at indicated time points. GAPDH levels were used as loading control. The length of uXBP1 is 204 bp and that of sXBP1 is 178 bp. (D) qRT-PCR analysis of the expression of ATF4, CHOP, and Bcl-2 during PRV infection. Mock-infected cells were used as controls.

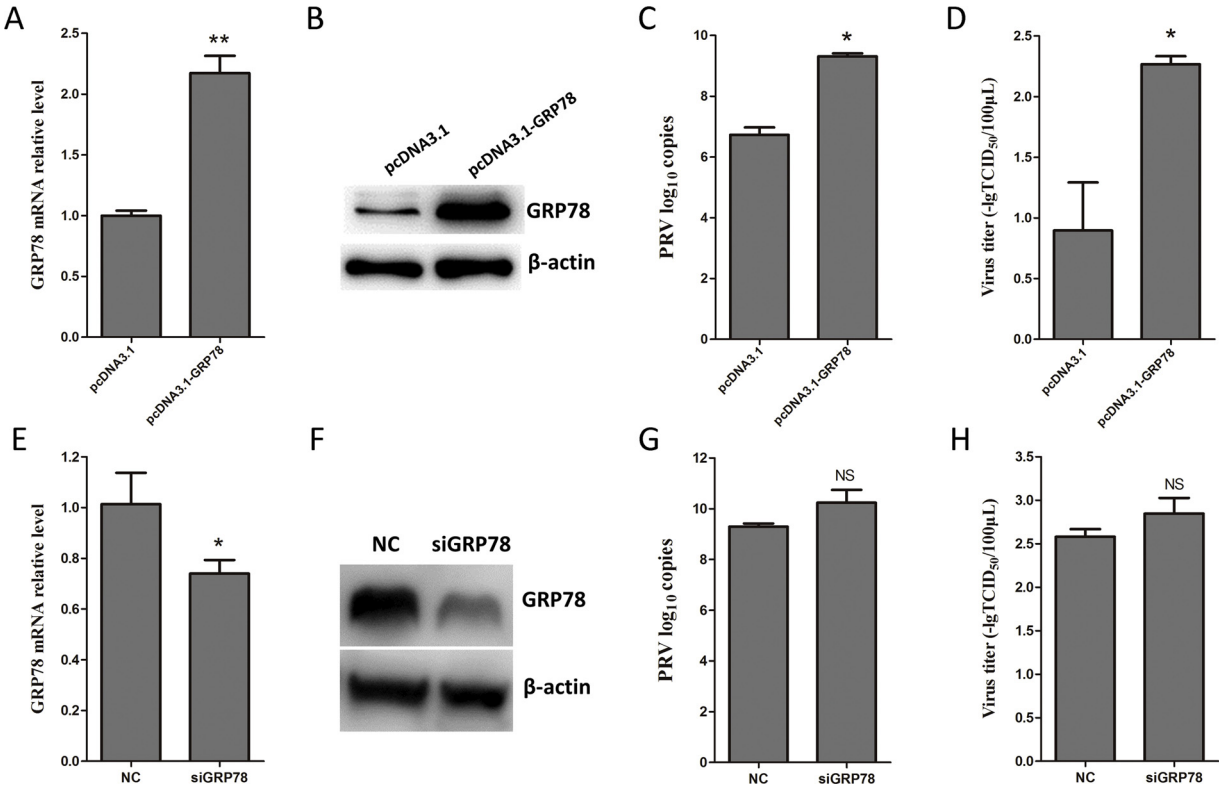

Fig. 4. Effects of overexpression and knockdown of GRP78 on PRV infection. PK15 cells were transfected with GRP78-expressing vector (pcDNA3.1) or GRP78-specific siRNA (siGRP78). Empty vector (pcDNA3.1) and scrambled RNA (NC) were used as negative controls. At 48 h post-transfection, the cells were infected with PRV for 12 h. qRT-PCR analysis of GRP78 mRNA levels in cells with GRP78 overexpression (A) or knockdown (E). Western blot analysis of GRP78 protein levels in cells with GRP78 overexpression (B) or knockdown (F). PRV replication (C) and production (D), measured by absolute qPCR and titer determination methods, respectively, in cells with GRP78 overexpression. PRV replication (G) and production (H) in cells with GRP78 knockdown.

enhanced PRV replication and virus production. To further understand the roles of GRP78 in PRV infection, we then performed a knockdown of GRP78 expression using siRNA. siRNA knockdown efficiency was confirmed by qRT-PCR and western blotting (Fig. 4E, F). Interestingly, knockdown of GRP78 expression did not significantly impact PRV replication or titers (Fig. 4G, H).

3.5. Chemical modification of ER stress and its effect on PRV infection

To further investigate the roles of ER stress on PRV replication, ER stress inducer Tg and inhibitor TUDCA were used. PK15 cells were treated with Tg or TUDCA at different concentrations for 4 h. Tg was removed through washing with PBS, and the treated cells were then infected with PRV for 12 h, whereas TUDCA remained during the viral infection. The DNA of the infected cells were extracted for absolute qPCR, and the supernatants were harvested for TCID50 assays. The results showed that GRP78 protein levels significantly increased in Tg-treated cells compared to untreated cells (Fig. 5A). Tg treatment did not affect cell viability (Fig. 5B). Absolute qPCR and TCID50 assays showed that low concentration of Tg (0.01 μM, 0.05 μM, and 0.1 μM) treatments significantly increased PRV replication and virus yield (Fig. 5C, D); however, treatment with high concentration of Tg (0.5 μM, 1 μM, and 2 μM) significantly inhibited PRV replication and virus yield (Supplemental Fig. 3). TUDCA treatment downregulated the GRP78 expression and thereby inhibited ER stress (Fig. 5E). TUDCA treatment had no effect on cell viability (Fig. 5F). PRV replication and titer were decreased in TUDCA-treated cells compared to untreated cells (Fig. 5G, H). Additionally, treatment with dithiothreitol (DTT), another ER stress inducer, slightly reduced PRV replication (Supplemental Fig. 4).

4. Discussion

Accumulating studies have shown that ER stress is induced and UPR is activated during viral infection because of the large amount of viral proteins that accumulate in the ER lumen (Chan, 2014; Zhang and Wang, 2012). Compared to DNA viruses, RNA viruses have been better characterized for their activation of the three branches of the UPR (Blazquez et al., 2014; Jheng et al., 2014). HSV1 is a member of the *Herpesviridae* family, and several studies have implicated the involvement of ER stress in HSV1 infection. HSV1 triggers the activation of PERK and mediates eIF-2alpha dephosphorylation (Cheng et al., 2005). gB regulates viral protein accumulation through an association with PERK to maintain ER homeostasis (Mulvey et al., 2007). HSV1 was found to effectively disarm the UPR in early stages of viral infection and activate the eIF2α/ATF4 signaling pathway at the final stage of HSV1 replication (Burnett et al., 2012). The HSV1 UL41 protein suppresses the IRE1-XBP1 signaling pathway via its RNase activity during infection (Zhang et al., 2017). Although PRV is also a member of the *Herpesviridae* family, it previously remained unknown whether PRV infection similarly involved ER stress induction and UPR activation. Several studies of PRV infection have been carried out on PK15 cells (Huang et al., 2014; Li et al., 2019; Yang et al., 2017). In addition, PRV infection of PK15 cells can cause obvious CPEs. Therefore, PK15 cells are considered an appropriate model for the study of host cell-PRV interactions. We examined the kinetics of PRV propagation in PK15 cells. An obvious CPE was visible at 24 hpi, and the viral titer dramatically increased and peaked at 24 hpi. These results were consistent with our previous study, suggesting that PRV infection could lead to rapid and severe CPE in PK15 cells (Yang et al., 2017).

GRP78 sensor is a marker of ER stress. The expression of GRP78 was significantly upregulated from 2 to 8 hpi and decreased from 1 2 to 24 h

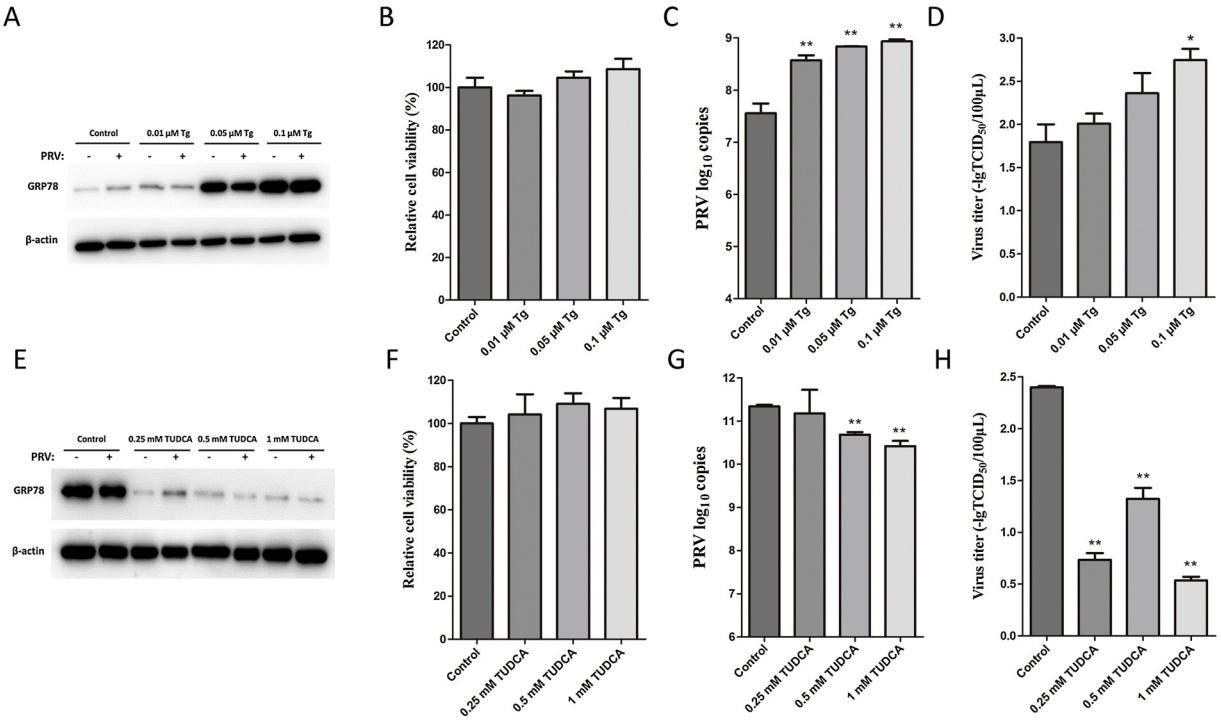

Fig. 5. Chemical modification of ER stress affects PRV infection. PK15 cells were treated with Tg at concentrations of 0.01 μM, 0.05 μM, and 0.1 μM for 4 h. The Tg was then removed and the cells were infected with PRV for 12 h. (A) The expression of GRP78 detected by western blotting, using mock-infected cells as controls. (B) Cell viability measured using CCK-8 as described in Materials and methods. (C) PRV replication levels analyzed by absolute qPCR. (D) Viral production levels measured by TCID50. PK15 cells were treated with TUDCA at concentrations of 0.25 mM, 0.5 mM, and 1 mM for 4 h. The cells were then infected with PRV for 12 h, with TUDCA present during the viral infection. (E) The expression of GRP78 detected by western blotting. (F) Cell viability measured using CCK-8. (G) PRV replication levels analyzed by absolute qPCR. (H) Viral production levels measured by TCID50.

pi. These results demonstrated that PRV induced ER stress at early infection stages. GRP78 works not only as a molecular chaperone to help unfolded viral proteins to fold properly but also as a cellular receptor to mediate viral entry (Buchkovich et al., 2009; Gething and Sambrook, 1992; Nain et al., 2017; Zhao et al., 2018). Therefore, PRV may interact with GRP78 to facilitate viral infection at early stages, subsequently inhibiting the expression of GRP78 to avoid severe ER stress and to maintain ER balance. The functional roles of GRP78 were examined through ectopic and knockdown expression studies. PRV replication and titer were increased after GRP78 overexpression, suggesting that GRP78 may improve the efficiency of viral entry and assembly to enhance viral infection. However, the viral replication and titer did not significantly change after knockdown of GRP78 expression. Logically speaking, the overexpression and knockdown of GRP78 should have opposite effects on viral expression (He et al., 2017; Zhao et al., 2018; Zhou et al., 2016). Because GRP78 is multifunctional, we speculated that knockdown of GRP78 expression may activate the expression of other molecular chaperones, such as GRP94, CANX, and CALR, the levels of which were found to be increased during PRV infection in our previous study (Yang et al., 2017). Therefore, the upregulated expression of these genes could compensate for the effects of GRP78 knockdown. Additional research is required to investigate the particular functions of GRP78 during PRV infection.

We also examined the three arms of the UPR during PRV infection. Among the three stress sensors, the IRE1-XBP1 pathway is the most conserved branch, and phosphorylated IRE1 splices the XBP1 mRNA to form sXBP1 mRNA during ER stress (Hetz et al., 2011). In the present study, the phosphorylation level of IRE1 was increased from 4 hpi to 24 hpi. In addition, sXBP1 mRNA was not detectable before infection but increased during PRV infection. These results demonstrate that the IRE1-XBP1 pathway was activated during PRV infection. In the early stage of infection, flaviviruses activated IRE1-XBP1 pathway to reduce cytotoxicity. The activation of IRE1-XBP1 pathway could enhance protein-folding ability through increasing expression of molecular chaperones, and it also could reduce ER loads by enhancing protein-degradation ability (Yu et al., 2006). Interestingly, in HSV1-infected cells, the viral UL41 protein suppresses the IRE1-XBP1 pathway to avoid cellular stress responses that may be harmful to viral replication (Zhang et al., 2017). Therefore, we speculate that PRV may activate the IRE1-XBP1 pathway to facilitate viral infection. In order to validate our speculation, siRNAs were used to knockdown the expression of IRE1 and XBP1 gene and infected with PRV. However, PRV replication did not significantly change after knockdown of IRE1 or XBP1 expression. Similarly with our results, the flavivirus production did not significantly changed after XBP1 knockdown (Yu et al., 2006). We speculate that IRE1-XBP1 pathway is not essential for PRV infection or the endogenous level of p-IRE1 and sXBP1 did not changed after knockdown of the expression of IRE1 or XBP1 using siRNA. The exact role of IRE1-XBP1 pathway in PRV infection needs to be further investigated. Generally speaking, viral replication and a large number of viral proteins accumulation in host cells could lead to ER stress. Interestingly, in the present study, PRV replication and viral particles could be examined as early as 2hpi. However, the viral proteins could not be detected until at 24hpi. Therefore, It is possible that there are other endogenous imbalances induce ER stress and UPR during PRV infection. For example, CSFV activated the IRE1 signal during viral entry stage through inhibiting cytoplasm Ca2+ level rather than viral protein accumulation (He et al., 2017). The molecular mechanism of UPR activation during early stages of PRV infection needs to be further investigated.

The activation of the PERK pathway is the most immediate response to the accumulation of unfolded proteins. Therefore, in order to alleviate ER stress, the PERK pathway is activated and eIF2α is phosphorylated to reduce translation of both cellular and viral mRNA (Fribley et al., 2009; Wek et al., 2006). However, if ER stress is prolonged or severe, ATF4, the downstream target of the PERK pathway, will induce the expression of CHOP to mediate cell apoptosis (Ron and

Walter, 2007; Tabas and Ron, 2011). In the present study, the levels of phosphorylated eIF2α were up-regulated at 2 hpi and 24hpi compared to the levels in mock-infected cells. ATF4 expression was significantly increased during the entirety of the PRV infection. Unfortunately, we could not find appropriate antibody for porcine PERK. Therefore, we speculate that PRV infection could activate the PERK-eIF2α-ATF4 pathway. In line with this notion, the expression of CHOP was upregulated immediately after PRV infection and increased up to 29-fold at 24 hpi. Additionally, expression of the survival protein Bcl2, a downstream target of CHOP (McCullough et al., 2001), significantly decreased at 24 hpi. The activation of the CHOP-Bcl2 pathway may lead to cell apoptosis, and, indeed, obvious CPE was visible at 24 hpi. These results demonstrated that PRV infection may activate the PERK-eIF2α-ATF4-CHOP-Bcl-2 pathway to induce apoptosis at late stages of infection.

The battle between host cell and virus begins when the virus enters the cell. On the one hand, viral infection induces ER stress due to the accumulation of a large number of viral proteins in the ER lumen. Additionally, the virus can control the ER stress response and induce the UPR to benefit viral protein folding and viral replication. On the other hand, the outcomes of the UPR, such as attenuated translation, ERAD and apoptosis, can limit viral replication (Chan, 2014). Growing studies have shown that virus-induced ER stress regulates viral replication (Fink et al., 2017; Galindo et al., 2012; Nair et al., 2016). To explore the roles of ER stress in PRV infection, the effects of two chemicals, Tg and TUDCA, on PRV infection was also examined. Tg is well known as an ER stress inducer that inhibits ER Ca^{2+}-ATPase and results in the depletion of calcium from the ER lumen (Hiroi et al., 2005; Thastrup et al., 1990). TUDCA is an effective ER stress inhibitor and alleviates ER stress and blocks apoptosis (Yoon et al., 2016; Zhang et al., 2018). In our study, treatment with Tg or TUDCA significantly increased or reduced the expression of GRP78, respectively. Accordingly, treatment with Tg or TUDCA significantly increased or reduced PRV replication and production. These results demonstrate that ER stress is favorable for PRV infection. Interestingly, the high concentrations of Tg treatment reduced PRV replication. We supposed that the high concentrations of Tg resulted in severe ER stress, which is harmful to viral infection (He et al., 2017). Similarly, treatment with DTT slightly reduced PRV replication. Although DTT could induce ER stress through inhibiting disulfide bond formation of newly synthesized proteins (Braakman et al., 1992), its function is broad and relatively unspecific as a strong reducing agent. We speculated that the pro-apoptotic effect of DTT may be detrimental to PRV infection.

Declaration of Competing Interest

The authors declare that they have no conflict of interest.

Acknowledgments

This work was supported by the Zhejiang Provincial Natural Science Foundation of China (LY19C170002). We acknowledge Cun Zhang (Zhejiang Academy of Agricultural Science, Hangzhou, China) for generously providing the PRV ZJ strain.

Appendix A. Supplementary data

Supplementary material related to this article can be found, in the online version, at doi:https://doi.org/10.1016/j.vetmic.2019.108485.

References

Blazquez, A.B., Escribano-Romero, E., Merino-Ramos, T., Saiz, J.C., Martin-Acebes, M.A., 2014. Stress responses in flavivirus-infected cells: activation of unfolded protein response and autophagy. Front. Microbiol. 5, 266.
Braakman, I., Helenius, J., Helenius, A., 1992. Manipulating disulfide bond formation and protein folding in the endoplasmic reticulum. EMBO J. 11, 1717–1722.
Buchkovich, N.J., Maguire, T.G., Paton, A.W., Paton, J.C., Alwine, J.C., 2009. The endoplasmic reticulum chaperone BiP/GRP78 is important in the structure and function of the human cytomegalovirus assembly compartment. J. Virol. 83, 11421–11428.
Burnett, H.F., Audas, T.E., Liang, G., Lu, R.R., 2012. Herpes simplex virus-1 disarms the unfolded protein response in the early stages of infection. Cell Stress Chaperones 17, 473–483.
Cai, Y., Arikkath, J., Yang, L., Guo, M.L., Periyasamy, P., Buch, S., 2016. Interplay of endoplasmic reticulum stress and autophagy in neurodegenerative disorders. Autophagy 12, 225–244.
Calfon, M., Zeng, H., Urano, F., Till, J.H., Hubbard, S.R., Harding, H.P., Clark, S.G., Ron, D., 2002. IRE1 couples endoplasmic reticulum load to secretory capacity by processing the XBP-1 mRNA. Nature 415, 92–96.
Chan, S.W., 2014. The unfolded protein response in virus infections. Front. Microbiol. 5, 518.
Cheng, G., Feng, Z., He, B., 2005. Herpes simplex virus 1 infection activates the endoplasmic reticulum resident kinase PERK and mediates eIF-2alpha dephosphorylation by the gamma(1)34.5 protein. J. Virol. 79, 1379–1388.
Fink, S.L., Jayewickreme, T.R., Molony, R.D., Iwawaki, T., Landis, C.S., Lindenbach, B.D., Iwasaki, A., 2017. IRE1alpha promotes viral infection by conferring resistance to apoptosis. Sci. Signal. 10.
Fribley, A., Zhang, K., Kaufman, R.J., 2009. Regulation of apoptosis by the unfolded protein response. Methods Mol. Biol. 559, 191–204.
Galindo, I., Hernaez, B., Munoz-Moreno, R., Cuesta-Geijo, M.A., Dalmau-Mena, I., Alonso, C., 2012. The ATF6 branch of unfolded protein response and apoptosis are activated to promote African swine fever virus infection. Cell Death Dis. 3, e341.
Gething, M.J., Sambrook, J., 1992. Protein folding in the cell. Nature 355, 33–45.
Gu, Z., Hou, C., Sun, H., Yang, W., Dong, J., Bai, J., Jiang, P., 2015. Emergence of highly virulent pseudorabies virus in southern China. Can. J. Vet. Res. 79, 221–228.
He, W., Xu, H., Gou, H., Yuan, J., Liao, J., Chen, Y., Fan, S., Xie, B., Deng, S., Zhang, Y., Chen, J., Zhao, M., 2017. CSFV infection up-regulates the unfolded protein response to promote its replication. Front. Microbiol. 8, 2129.
Hetz, C., Martinon, F., Rodriguez, D., Glimcher, L.H., 2011. The unfolded protein response: integrating stress signals through the stress sensor IRE1alpha. Physiol. Rev. 91, 1219–1243.
Hiroi, T., Wei, H., Hough, C., Leeds, P., Chuang, D.M., 2005. Protracted lithium treatment protects against the ER stress elicited by thapsigargin in rat PC12 cells: roles of intracellular calcium, GRP78 and Bcl-2. Pharmacogenomics J. 5, 102–111.
Huang, J., Ma, G., Fu, L., Jia, H., Zhu, M., Li, X., Zhao, S., 2014. Pseudorabies viral replication is inhibited by a novel target of miR-21. Virology 456–457, 319–328.
Ibrahim, I.M., Abdelmalek, D.H., Elfiky, A.A., 2019. GRP78: a cell's response to stress. Life Sci. 226, 156–163.
Jheng, J.R., Ho, J.Y., Horng, J.T., 2014. ER stress, autophagy, and RNA viruses. Front. Microbiol. 5, 388.
Klupp, B.G., Hengartner, C.J., Mettenleiter, T.C., Enquist, L.W., 2004. Complete, annotated sequence of the pseudorabies virus genome. J. Virol. 78, 424–440.
Lee, A.H., Iwakoshi, N.N., Glimcher, L.H., 2003. XBP-1 regulates a subset of endoplasmic reticulum resident chaperone genes in the unfolded protein response. Mol. Cell. Biol. 23, 7448–7459.
Lee, A.S., 2005. The ER chaperone and signaling regulator GRP78/BiP as a monitor of endoplasmic reticulum stress. Methods 35, 373–381.
Li, X., Zhang, W., Liu, Y., Xie, J., Hu, C., Wang, X., 2019. Role of p53 in pseudorabies virus replication, pathogenicity, and host immune responses. Vet. Res. 50, 9.
Livak, K.J., Schmittgen, T.D., 2001. Analysis of relative gene expression data using real-time quantitative PCR and the 2(-Delta Delta C(T)) method. Methods 25, 402–408.
McCullough, K.D., Martindale, J.L., Klotz, L.O., Aw, T.Y., Holbrook, N.J., 2001. Gadd153 sensitizes cells to endoplasmic reticulum stress by down-regulating Bcl2 and perturbing the cellular redox state. Mol. Cell. Biol. 21, 1249–1259.
Muller, T., Hahn, E.C., Tottewitz, F., Kramer, M., Klupp, B.G., Mettenleiter, T.C., Freuling, C., 2011. Pseudorabies virus in wild swine: a global perspective. Arch. Virol. 156, 1691–1705.
Mulvey, M., Arias, C., Mohr, I., 2007. Maintenance of endoplasmic reticulum (ER) homeostasis in herpes simplex virus type 1-infected cells through the association of a viral glycoprotein with PERK, a cellular ER stress sensor. J. Virol. 81, 3377–3390.
Nain, M., Mukherjee, S., Karmakar, S.P., Paton, A.W., Paton, J.C., Abdin, M.Z., Basu, A., Kalia, M., Vrati, S., 2017. GRP78 is an important host factor for Japanese encephalitis virus entry and replication in mammalian cells. J. Virol. 91.
Nair, V.P., Anang, S., Subramani, C., Madhvi, A., Bakshi, K., Srivastava, A., Shalimar, Nayak, B., Ranjith Kumar, C.T., Surjit, M., 2016. Endoplasmic reticulum stress induced synthesis of a novel viral factor mediates efficient replication of Genotype-1 hepatitis E virus. PLoS Pathog. 12, e1005521.
Oyadomari, S., Mori, M., 2004. Roles of CHOP/GADD153 in endoplasmic reticulum stress. Cell Death Differ. 11, 381–389.
Pomeranz, L.E., Reynolds, A.E., Hengartner, C.J., 2005. Molecular biology of pseudorabies virus: impact on neurovirology and veterinary medicine. Microbiol. Mol. Biol. Rev. 69, 462–500.
Ron, D., Walter, P., 2007. Signal integration in the endoplasmic reticulum unfolded protein response. Nat. Rev. Mol. Cell Biol. 8, 519–529.
Schroder, M., Kaufman, R.J., 2005. The mammalian unfolded protein response. Annu. Rev. Biochem. 74, 739–789.
Sharma, M., Bhattacharyya, S., Sharma, K.B., Chauhan, S., Asthana, S., Abdin, M.Z., Vrati, S., Kalia, M., 2017. Japanese encephalitis virus activates autophagy through XBP1 and ATF6 ER stress sensors in neuronal cells. J. Gen. Virol. 98, 1027–1039.
Sun, M., Hou, L., Tang, Y.D., Liu, Y., Wang, S., Wang, J., Shen, N., An, T., Tian, Z., Cai, X., 2017. Pseudorabies virus infection inhibits autophagy in permissive cells in vitro. Sci. Rep. 7, 39964.

Tabas, I., Ron, D., 2011. Integrating the mechanisms of apoptosis induced by endoplasmic reticulum stress. Nat. Cell Biol. 13, 184–190.
Thastrup, O., Cullen, P.J., Drobak, B.K., Hanley, M.R., Dawson, A.P., 1990. Thapsigargin, a tumor promoter, discharges intracellular Ca2+ stores by specific inhibition of the endoplasmic reticulum Ca2(+)-ATPase. Proc. Natl. Acad. Sci. U. S. A. 87, 2466–2470.
Verpoest, S., Cay, A.B., De Regge, N., 2014. Molecular characterization of Belgian pseudorabies virus isolates from domestic swine and wild boar. Vet. Microbiol. 172, 72–77.
Walter, P., Ron, D., 2011. The unfolded protein response: from stress pathway to homeostatic regulation. Science 334, 1081–1086.
Wek, R.C., Jiang, H.Y., Anthony, T.G., 2006. Coping with stress: eIF2 kinases and translational control. Biochem. Soc. Trans. 34, 7–11.
Xu, C., Wang, M., Song, Z., Wang, Z., Liu, Q., Jiang, P., Bai, J., Li, Y., Wang, X., 2018. Pseudorabies virus induces autophagy to enhance viral replication in mouse neuro-2a cells in vitro. Virus Res. 248, 44–52.
Yang, S., Pei, Y., Zhao, A., 2017. iTRAQ-based proteomic analysis of porcine kidney epithelial PK15 cells infected with pseudorabies virus. Sci. Rep. 7, 45922.
Yoon, Y.M., Lee, J.H., Yun, S.P., Han, Y.S., Yun, C.W., Lee, H.J., Noh, H., Lee, S.J., Han, H.J., Lee, S.H., 2016. Tauroursodeoxycholic acid reduces ER stress by regulating of Akt-dependent cellular prion protein. Sci. Rep. 6, 39838.
Yu, C.Y., Hsu, Y.W., Liao, C.L., Lin, Y.L., 2006. Flavivirus infection activates the XBP1 pathway of the unfolded protein response to cope with endoplasmic reticulum stress. J. Virol. 80, 11868–11880.
Yu, X., Zhou, Z., Hu, D., Zhang, Q., Han, T., Li, X., Gu, X., Yuan, L., Zhang, S., Wang, B., Qu, P., Liu, J., Zhai, X., Tian, K., 2014. Pathogenic pseudorabies virus, China, 2012. Emerg. Infect. Dis. 20, 102–104.
Zhang, K., Kaufman, R.J., 2004. Signaling the unfolded protein response from the endoplasmic reticulum. J. Biol. Chem. 279, 25935–25938.
Zhang, L., Wang, A., 2012. Virus-induced ER stress and the unfolded protein response. Front. Plant Sci. 3, 293.
Zhang, P., Su, C., Jiang, Z., Zheng, C., 2017. Herpes simplex virus 1 UL41 protein suppresses the IRE1/XBP1 signal pathway of the unfolded protein response via its RNase activity. J. Virol. 91.
Zhang, Y., Qu, P., Ma, X., Qiao, F., Ma, Y., Qing, S., Wang, Y., Cui, W., 2018. Tauroursodeoxycholic acid (TUDCA) alleviates endoplasmic reticulum stress of nuclear donor cells under serum starvation. PLoS One 13, e0196785.
Zhao, D., Liu, Q., Han, K., Wang, H., Yang, J., Bi, K., Liu, Y., Liu, N., Tian, Y., Li, Y., 2018. Identification of glucose-regulated Protein 78 (GRP78) as a receptor in BHK-21 cells for duck tembusu virus infection. Front. Microbiol. 9, 694.
Zhou, Y., Qi, B., Gu, Y., Xu, F., Du, H., Li, X., Fang, W., 2016. Porcine circovirus 2 deploys PERK pathway and GRP78 for its enhanced replication in PK-15 cells. Viruses 8.